AGU PUBLICATIONS

Geophysical Research Letters

RESEARCH LETTER
10.1002/2014GL060140

Key Points:
- Fast grounding line retreat of the entire Amundsen Sea sector of West Antarctica
- Observations are a signature of a marine ice sheet instability in Antarctica
- This sector of Antarctica will remain the largest contributor to sea level rise

Supporting Information:
- Readme
- Figure S1
- Figure S2–S6
- Figure S7
- Figure S8
- Figure S9
- Figure S10

Correspondence to:
E. Rignot,
erignot@uci.edu

Citation:
Rignot, E., J. Mouginot, M. Morlighem, H. Seroussi, and B. Scheuchl (2014), Widespread, rapid grounding line retreat of Pine Island, Thwaites, Smith, and Kohler glaciers, West Antarctica, from 1992 to 2011, *Geophys. Res. Lett.*, *41*, 3502–3509, doi:10.1002/2014GL060140.

Received 6 APR 2014
Accepted 3 MAY 2014
Accepted article online 12 MAY 2014
Published online 27 MAY 2014

Widespread, rapid grounding line retreat of Pine Island, Thwaites, Smith, and Kohler glaciers, West Antarctica, from 1992 to 2011

E. Rignot[1,2], J. Mouginot[1], M. Morlighem[1], H. Seroussi[2], and B. Scheuchl[1]

[1]Department of Earth System Science, University of California, Irvine, California, USA, [2]Jet Propulsion Laboratory, California Institute of Technology, Pasadena, California, USA

Abstract We measure the grounding line retreat of glaciers draining the Amundsen Sea sector of West Antarctica using Earth Remote Sensing (ERS-1/2) satellite radar interferometry from 1992 to 2011. Pine Island Glacier retreated 31 km at its center, with most retreat in 2005–2009 when the glacier ungrounded from its ice plain. Thwaites Glacier retreated 14 km along its fast flow core and 1 to 9 km along the sides. Haynes Glacier retreated 10 km along its flanks. Smith/Kohler glaciers retreated the most, 35 km along its ice plain, and its ice shelf pinning points are vanishing. These rapid retreats proceed along regions of retrograde bed elevation mapped at a high spatial resolution using a mass conservation technique that removes residual ambiguities from prior mappings. Upstream of the 2011 grounding line positions, we find no major bed obstacle that would prevent the glaciers from further retreat and draw down the entire basin.

1. Introduction

The grounding line is the critical boundary between grounded ice and the ocean which delineates where ice detaches from the bed and becomes afloat and frictionless at its base. Its position is mapped accurately (millimeter of vertical motion), at a high spatial resolution (< 50 m), simultaneously and uniquely over large areas using satellite radar interferometry (interferometric synthetic aperture radar (InSAR)) [*Rignot et al.*, 2011]. Knowledge of this position is critical for mass flux calculation and mass budget assessment [e.g., *Rignot et al.*, 2008], ice sheet numerical modeling [e.g., *Larour et al.*, 2012; *Gillet-Chaulet and Durand*, 2010], analysis of ice shelf melting [*Rignot et al.*, 2013], and evaluation of glacier/ice shelf stability [*Thomas et al.*, 2004a, 2004b]. In the Amundsen Sea (AS) sector of West Antarctica, grounding line mapping has revealed major glacier changes in the 1990s [*Rignot*, 1998, 2001], subsequently confirmed by satellite radar altimetry [*Wingham et al.*, 2009], laser altimetry [*Pritchard et al.*, 2009] and time-variable gravity [*Velicogna and Wahr*, 2006]. The AS is a dominant contributor to the mass loss from the Antarctic ice sheet at present, with losses driven almost entirely by increases in flow speed [*Mouginot et al.*, 2014]. This sector is of global significance since it contains enough ice to raise global sea level by 1.2 m [e.g., *Rignot*, 2008].

Here we present and analyze observations of grounding line retreat for all the glaciers draining into the AS from 1992 to 2011. We compare the observed pattern of grounding line retreat with two bed topographies: (1) the recent BEDMAP-2 topography [*Fretwell et al.*, 2013] and (2) a new, improved topography that combines ice thickness with ice motion vector using a mass conservation (MC) optimization [*Morlighem et al.*, 2011, 2013]. We discuss the results and draw conclusions on the evolution of this major sector of West Antarctica.

2. Data and Methods

We use InSAR data from the European Earth Remote Sensing (ERS-1/2) radar satellite (5.6 cm wavelength) collected in 1992 and 1994 (3 day repeat), ERS-1 and ERS-2 tandem data from 1996 (Figure 1) and 2000 (1 day repeat), and ERS-2 from 2011 (3 day repeat). We employ a quadruple differential InSAR technique [*Rignot et al.*, 2011] where interferograms spanning the same time interval and corrected for surface topography are differenced to measure the short-term, meter-scale vertical motion of the ice forced by changes in oceanic tides.

Starting in 2001, ERS-2 had to operate without its gyroscopes. This made it difficult to control the antenna pointing and yielded data with severe drifts in Doppler centroid along track. To maintain InSAR coherence,

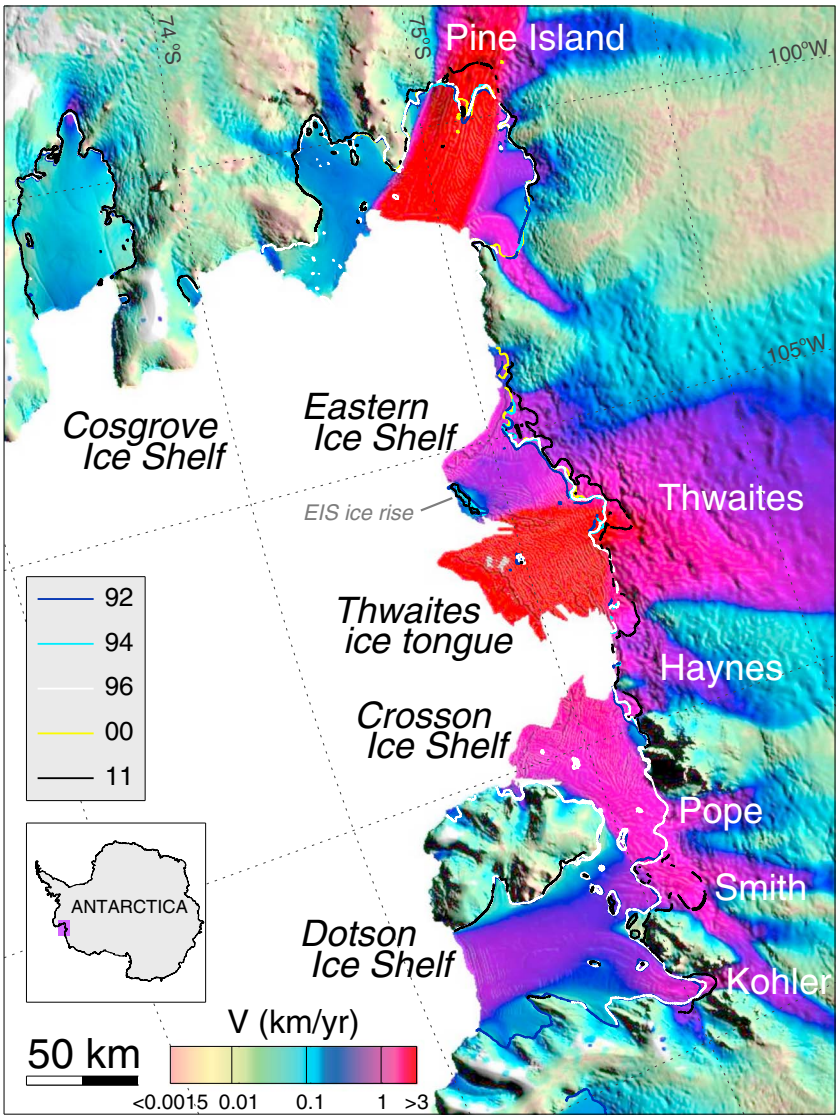

Figure 1. Velocity of the Amundsen Sea (AS) sector of West Antarctica derived using ERS-1/2 radar data in winter 1996 with a color coding on a logarithmic scale and overlaid on a Moderate Resolution Imaging Spectroradiometer mosaic of Antarctica. Interferometrically derived grounding lines of the glaciers are shown in color code for years 1992, 1994, 1996, 2000, and 2011, with glacier and ice shelf names. Note that for Pine Island and Smith/Kohler, the figure merges two independent differential interferograms to show a more complete spatial coverage of grounding lines.

we select ERS-2 pairs with the same rate of along-track drift in Doppler centroid estimated by processing small segments of acquired data. We use data collected in spring 2011 when the European Space Agency moved ERS-2 back to a 3 day repeat cycle to enable grounding line mapping of fast-moving glaciers. In July 2011, ERS-2 terminated its mission after 16 years of services, far exceeding its planned operational lifespan.

To pick grounding lines, we map the inward limit of detection of vertical motion, where the glacier lifts off the bed and becomes afloat (Figure 2). We do not use an elastic model to detect the hinge-line position [e.g., *Park et al.*, 2013] because of the following: (1) this inversion requires a two-dimensional viscoelastic model of tidal bending with spatially variable ice thickness and time-dependent hinge-line position; (2) the hinge line is not relevant for glacier stability and is not in hydrostatic equilibrium; and (3) InSAR fringes provide easier-to-extract, direct information on grounding line position. As grounding lines migrate back and forth with oceanic tides, we repeat the mapping multiple times with independent interferograms.

To interpret the pattern of retreat, we consider the pattern of ice motion (Figure 1) and bed topography (Figure 3). In the AS sector, BEDMAP-2's topography [*Fretwell et al.*, 2013] uses ice thickness data from the

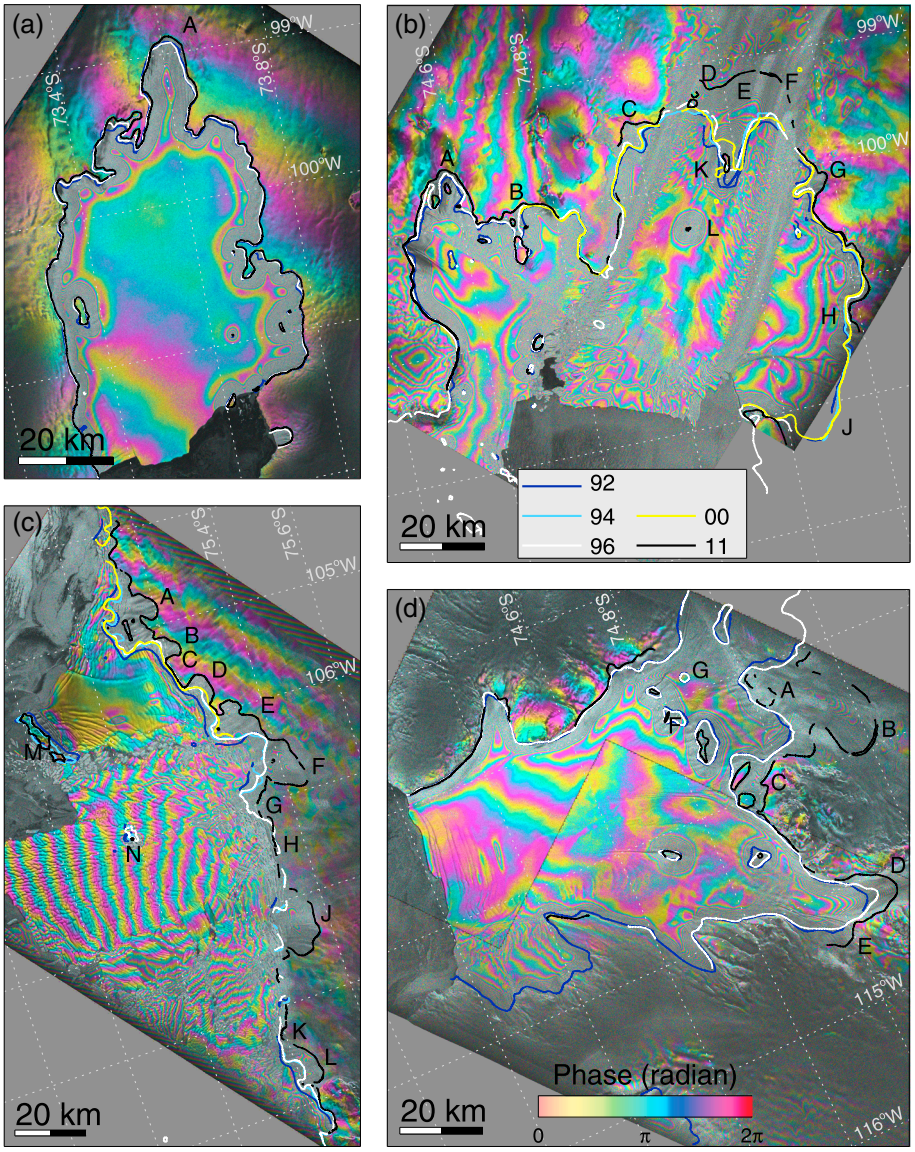

Figure 2. Differential interferograms of the tidal-induced vertical motion of (a) Cosgrove Ice Shelf on 1-4-7 April 2011, (b) Pine Island Glacier on 18-24-27 April 2011, (c) Thwaites Glacier on 1-4-7 April 2011, and (d) Smith/Kohler glaciers on 6-12/15-18 April 2011. Each color cycle is a 360 cycle in interferometric phase equivalent to a 28 mm motion of the surface in the direction of illumination of the radar. The grounding line is located at the inward limit of the tidally induced vertical motion. Letters in the figure refer to areas discussed in the text.

2002 NASA/CECS [*Thomas et al.*, 2004b], the 2004 BBAS/AGASEA [*Holt et al.*, 2006] and the 2009-2010-2011 NASA's Operation IceBridge surveys [*Gogineni*, 2012]. Thickness data from these different time periods were interpolated onto a regular grid at 1 km spacing using kriging.

We combine the ice velocity from ERS-1/2 1996 [*Mouginot et al.*, 2014] (Figure 1) with the BEDMAP-2 surface reference and the above mentioned ice thickness data to infer a new bed topography using an optimization algorithm that conserves mass [*Morlighem et al.*, 2011]. The MC technique provides bed and thickness products at the same resolution as the ice motion data (450 m), with minimal errors in ice flux divergence, lower interpolation errors compared to kriging, and a nominal error of 35–45 m [*Morlighem et al.*, 2013]. On Pine Island Glacier, the MC inversion reveals inconsistencies in the input data, which we discuss later on. A crossover analysis of the thickness data indicates a standard error of $\sigma = 83$ m within the MC domain (Figure 3), with most discrepancies between the 2002–2004 and 2009–2011 data. The error increases to

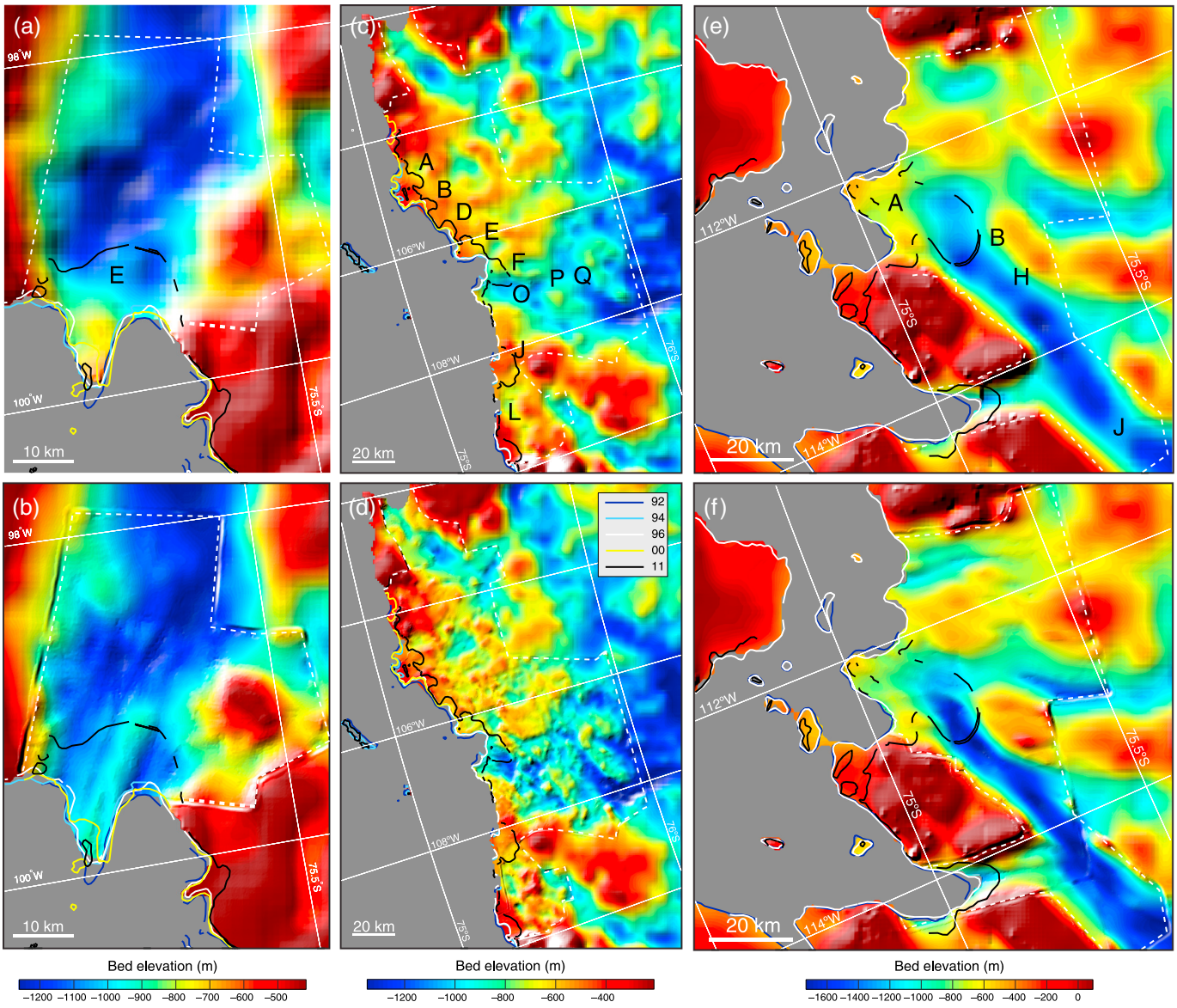

Figure 3. Bed topography (a, c, and e) from BEDMAP-2 and (b, d, and f) from a mass conservation (MC) algorithm for (Figures 3a and 3b) Pine Island, (Figures 3c and 3d) Thwaites and Haynes, (Figures 3e and 3f) Smith and Kohler glaciers in the Amundsen Sea (AS) sector of West Antarctica along with grounding line positions for 1992, 1994, 1996, 2000, and 2011. The limits of the MC domain are shown in white dotted line and extend to the grounding line. Outside of the MC domain, the bed topography is from BEDMAP-2.

150 m within a 15 km radius of the 1996 grounding line. For Smith/Kohler, σ = 132 m due to discrepancies between earlier and recent data. In contrast, on Thwaites, σ = 42 m and the MC optimization provides an excellent fit with the ice thickness observations.

As floating ice moves up and down with changes in oceanic tide, or grounding lines retreat over a rough bed, and if we assume that the basal water pressure is equal to the ice overburden pressure, seawater will infiltrate the glacier base along the lines of lowest hydrostatic potential (here expressed in meters), $\phi = Z_s + \frac{\rho_w - \rho_i}{\rho_i} Z_b$, where ρ_i is the density of ice (917 kg/m^3), ρ_w is the density of seawater (1028 kg/m^3), Z_s is the surface elevation, and Z_b is the bed elevation. In this expression, Z_b is factored by 0.12 but exhibits a larger variability than Z_s. Within the MC domain, bed slope has a mean 3 times larger and a standard deviation 10 times larger than surface slope (Figure S1 in the supporting information). On Pine Island, surface slope increases with time as a result of thinning, but the changes are small: 0.6 to 1.15 × 10^{-5} year^{-1} versus a mean slope of −0.00135, i.e., 0.4 to 0.9% year^{-1} or 8 to 16% in 19 years [*Scott et al.*, 2009]. Therefore,

surface elevation is smooth, bed elevation is rough, and both quantities do not change on the time scales considered here. Bed elevation is also most important for two other reasons: (1) the freezing point of seawater depends on water pressure, so the deeper the glacier bed the easier it is for seawater to melt glacier ice; and (2) glaciers grounded on a retrograde bed are inherently unstable; hence, it is essential to examine bed slopes when interpreting grounding line retreat. Our discussion thus focuses on bed elevation.

3. Results

The 1996 ice velocity (Figure 1) provides a visual reference for comparing the grounding line retreat with flow speed, because changes in flow speed are largest in fast-moving areas [*Mouginot et al.*, 2014], which therefore thin the most and are most conducive to ice ungrounding. The velocity data also help identify ice rises, which are grounded ice islands with zero ice motion, and separate them from ice rumples, where ice speed is nonzero as ice moves over a grounded area.

Differential interferograms and grounding lines are shown in Figure 2 for 2011 and Figures S2–S6 for other years. All retreat rates quoted below are measured along flow lines. The two 2011 grounding lines of Pine Island and Smith/Kohler glaciers agree to within 100–150 m; therefore, tidal fluctuations are 1 order of magnitude smaller than the decadal retreat rates considered herein. On Cosgrove Ice Shelf, we detect a 1 km retreat at the mouth of its main tributary (point A), but no migration elsewhere (Figure 2a). On Pine Island Glacier, the retreat is 31 km at the glacier center (point E in Figure 2b) and 7 to 10 km on the sides (D and F), i.e., the profile evolves from convex downstream to concave upstream. The migration decreases to zero at the side margins (inward of C and G), as noted by *Park et al.* [2013]. On the tributaries, grounding lines retreat as well, especially close to the main trunk of Pine Island: 1.4 km at point A, 0.9 km at B, but 8.5 km at C on the east side, 1.5 km at H but 10 km at G on the west side. We have no 2011 data on the stream merging into the ice shelf from the west at point K, but we detect no migration in 1992–2000. At L, an ice rumple 0.5 km in diameter appears in 2011. We attribute its appearance to the irregular advection of patches of thicker ice from upstream that are clearly seen in time series of visible imagery (Figure S7). An ice rumple, 1 km × 4 km in size, remains at the 1996 grounding line at K; a few other rumples disappeared or reduced in size on the northern ice shelf (near A and B).

Tidal fringes on Thwaites Glacier (Figure 2c) are of higher quality due to the absence of sharp shear margins and the availability of shorter-repeat interferograms. In the core of fast flow (Figure 1), the retreat is 12–18 km near F versus 2–7 km near G. Near H, the glacier is calving at the grounding line, migration is difficult to quantify due to the irregular nature of calving events. The retreat pattern is complex on the Eastern Ice Shelf (EIS) [*Mouginot et al.*, 2014]: 12–17 km at A, 7 km at B and D, 14 km at E, but 1 km at C. At A, the ice shelf is now twice longer since the ice front did not migrate. More significant is the evolution of the ice rise that buttresses EIS at M. The ice rise was 64 km^2 in area in 1992 and split into two ice elements with a total area of 31 km^2 in 2011. Assuming a basal shear stress uniform at 100 kPa—the yield stress of ice—the back force exerted by the ice rise on the EIS is now reduced by half [*Thomas*, 1973], which favors further speed up of EIS. On the ice tongue, an area of ephemeral grounding remains in 2011, indicating a shallow seafloor, but this feature has no impact on ice flow, as shown by *Schmeltz et al.* [2001].

Haynes Glacier is a distinct, smaller glacier west of Thwaites that calved at the grounding line in 1992 into a melange of stranded bergs, icebergs debris, and sea ice. The melange cleared up completely in early 2013 (Figure S8). At the center, near ice rise K, the glacier is still calving at the grounding line in 2011, migration is difficult to quantify but small; but between 1996 and 2011, a new ice shelf 150 km^2 in size formed at J (Figure 2b), via a 12 km grounding line retreat, and 100 km^2 at K via an 8 km retreat.

The most spectacular retreat is a 34–37 km migration at the center of Smith/Kohler glaciers (B in Figure 2d). Between A and B, ice was only a few 10 m above hydrostatic equilibrium in 2002 [*Thomas et al.*, 2004b]. A 500 km^2 region ungrounded from the bed in 1992–2011. On the sides of the ice stream, the retreat is 4 to 7 km. At C, in a region of low motion in the wake of Kohler Range, an 8 km retreat ungrounded an area of 100 km^2, with two new ice rises left. On the west branch of Kohler, the retreat is 8 km at D and 4 km at tributary E. The ice rumples between Crosson and Dotson ice shelves (area F) were 73 km^2 in area in 1992 and 15 km^2 in 2011, and one ice rumple disappeared at G. These observations imply that the ice shelf is thinning and unpinning from its anchoring points. ERS-2 did not image Pope Glacier in 2011, so its retreat is unquantified.

Examining the bed topography of Pine Island Glacier (Figures 3a and 3d), the MC bed is 150 to 350 m deeper than BEDMAP-2's near the 1996 grounding line (K). Radar echograms for the NASA data (echograms for other data are not available) (Figures S9–S10) reveal that bed returns are picked from an intermediate layer of bright echoes, which we attribute to hyperbolic echoes from bottom crevasses filled with seawater. A secondary layer of equally bright reflectors is found 150 to 350 m below that depth. We attribute this deeper layer to the draft of the water-filled bottom crevasses, at a bed elevation consistent with the MC results. The largest discrepancy is found near the grounding line, where water-filled bottom crevasses may indeed reach a large fraction of the total thickness [e.g., *MacGrath et al.*, 2012; *Weertman*, 1980]. The greater thickness in the MC map implies a surface elevation 15–35 m closer to floatation and hence easier to unground for a given thinning rate. Along the ice plain proper (K to E), the MC topography reveals a 4 km wide, 20 km long subglacial ridge that is not present in BEDMAP-2. Inland of the ridge, the bed decreases by several 100 m over the next 100 km.

On Thwaites Glacier (Figures 3b and 3e), MC and BEDMAP-2 are in good agreement (σ = 48 m versus 78 m on Pine Island), but the improvement in spatial resolution is significant. At A, the bed elevation is more uniformly deepening inland and conducive to retreat in MC than BEDMAP-2. At E, the MC bed is 100–150 m deeper and more consistent with a retreat. At F, the MC bed is deeper over a wider area, hence more favorable to retreat. At J, the MC is also 100 m deeper. Along the path of lowest bed elevation F-O-P-Q, the MC bed elevation is more rugged and detailed than BEDMAP-2. At O, P, and Q, the bed rises 100–250 m before decreasing 1200 m below sea level in a more uniformly deep basin.

On Smith/Kohler glaciers (Figures 3c and 3f), the 35 km retreat follows a deep trough that drops 800 m in elevation between A and B, and 100 m more in MC than in BEDMAP-2. Inland of B, the two topographies are comparable. The bed rises by 200 m at H and again at J. Beyond J, the bed remains 1600 m below sea level for another 40 km. Beneath Pope, the MC reveals a subglacial channel not present in BEDMAP-2. In contrast, on Kohler's west branch, the MC bed is 100–200 m shallower than in BEDMAP-2 and rising inland, hence represents the only sector in principle not favorable to rapid retreat.

4. Discussion

The analysis of bed topography reveals errors in BEDMAP-2 for Pine Island Glacier near its former grounding line. The MC approach helps identify these errors and improve the vertical accuracy and horizontal details of the bed topography. The BEDMAP-2 errors do not impact ice flux estimates obtained at the 2011 grounding line [*Mouginot et al.*, 2014] or at a 2002 crossing of the glaciers [*Rignot et al.*, 2008], but may affect recent modeling efforts that replicated the ungrounding of the ice plain and the glacier speed up [e.g., *Favier et al.*, 2014]. This emphasizes the importance of deriving improved bed topographies near the grounding lines of key glaciers to interpret the glacier retreat more precisely and subsequently improve the reliability of projections of ice flow evolution.

The grounding line retreat of Pine Island and Smith glaciers is constrained by the deep subglacial troughs beneath them. The change in grounding line profile from convex downstream to concave upstream indicates a faster thinning rate at the center, which is consistent with a larger increase in longitudinal stretching of ice at the center compared to the sides [*Mouginot et al.*, 2014]. In both areas, the grounding line migrated across a vast region of relatively shallow surface elevation above floatation, which facilitated a rapid ungrounding of 30–35 km of glacier length with a rate of ice thinning of only 3–5 m yr^{-1}. The retreat was accompanied by glacier speed up, as projected by *Thomas et al.* [2004a], due to the removal of basal friction as the ice plain ungrounded. Interestingly, the ice plain ungrounding occurred almost synchronously on both glaciers, which suggests that it was triggered by a common forcing, such as an increase in ocean heat flux in the AS in early 2000s that enhanced ice shelf melt [*Jacobs et al.*, 2011].

As a result of the retreat, Pine Island Glacier rested in 2011 on a bed 400 m deeper below sea level than in 1992, in a region where the bed elevation is smoothly decreasing inland, with no major hill to prevent further retreat. Stabilization could be achieved if ice shelf buttressing in the normal or transverse directions were to increase [*Jamieson et al.*, 2012; *Gudmundsson*, 2013], but the glacier becomes wider inland where tributaries merge, no bedrock high is present to initiate ice rise formation as the ice shelf retreats, and lateral shear along the margins is unlikely to become significant due to persistent cracking and rifting.

On Smith/Kohler glaciers, the ice stream in 2011 rested on a bed 800 m deeper below sea level than in 1992, at a depth where ocean thermal forcing is 0.6°C higher because of the pressure dependence of the melting point of sea ice, hence favorable to more vigorous ice shelf melt even if the ocean temperature does not change with time. Thicker ice at the onset of floatation experiences spreading rates enhanced by the cubic power of thickness [*Thomas*, 1973], i.e., ice flow will increase, ice will thin, and the retreat will continue. On the ice shelf proper, the pinning points are vanishing, with the consequence that the back force on the glacier is decreasing. Stabilization of the retreat could occur if the glacier were to retreat into a narrower valley, but the width of the subglacial valley remains constant over the next 50 km.

On Thwaites Glacier, the retreat rate is lower and more variable spatially because the glacier is not confined into a deep trough but rather expands across a 100 km wide landscape with rough basal topography. One deep channel underlays the fast flow core of Thwaites, while another projects into the adjacent ice shelf in front of Pine Island Glacier (K). Everywhere along the grounding line, the retreat proceeds along clear pathways of retrograde bed, with elevation dropping 1200 m below sea level. On this glacier, stabilization of the retreat from ice shelf buttressing is unlikely [*Parizek et al.*, 2013]. Upstream of the 2011 grounding line, the grounding line will keep retreating because of ongoing dynamic thinning. Only 2–3 ridges a few 100 m in height exist that may temporarily slow down the retreat.

In the east, the EIS is retreating and weakening, and its buttressing ice rise is vanishing. This evolution of EIS may have played a role in the recent acceleration of Thwaites since 2006, following decades of stability [*Mouginot et al.*, 2014]. If the EIS ice rise ceases its buttressing, the ice shelf will accelerate and the faster-moving portion of Thwaites will spread out laterally.

To the west, Haynes Glacier is an exception due to the presence of large mountain blocks at its center and upstream of the grounding line, but this glacier drains a small sector and its recent evolution is far from being an example of stabilization.

Since the 1970s, the AS ice discharge into the Southern Ocean has been increasing, especially in 2003–2008 when Pine Island and Smith/Kohler glaciers ungrounded from their ice plains, as documented by the abrupt change in speed during that time period [*Mouginot et al.*, 2014]. Ice flow changes are detected hundreds of kilometer inland, to the flanks of the topographic divides, demonstrating that coastal perturbations are felt far inland and propagate rapidly. As shown here, the glacier grounding lines retreat rapidly, at km/yr, over the entire sector. On Smith/Kohler, the retreat rate of 1.8 km/yr is even greater than its rate of horizontal motion of 1.1 km/yr. The retreats proceed, as expected, along deeper subglacial channels, and accelerate where the surface is at the onset of floatation. The grounding lines retreat dominantly on a retrograde bed, except for the west branch of Kohler, hence are inherently unstable, with no clear feature of stabilization upstream. These observations of change in velocity and grounding line retreat therefore concur with recent ice sheet model simulations to indicate that this sector of West Antarctica has developed a marine instability.

5. Conclusions

Using two decades of ERS-1/2 data, we document a continuous and rapid retreat of the grounding lines of Pine Island, Thwaites, Haynes, Smith, and Kohler glaciers, which drain a large sector of West Antarctica on a retrograde, submarine bed, a configuration deemed unstable by ice sheet numerical models [e.g., *Favier et al.*, 2014; *Katz and Worster*, 2010; *Parizek et al.*, 2013] unless normal and tangential ice shelf buttressing could increase significantly [*Gudmundsson*, 2013], which is unlikely. The retreat is proceeding along fast-flowing, accelerating sectors that are thinning, become bound to reach floatation and unground from the bed. We find no major bed obstacle upstream of the 2011 grounding lines that would prevent further retreat of the grounding lines farther south. We conclude that this sector of West Antarctica is undergoing a marine ice sheet instability that will significantly contribute to sea level rise in decades to centuries to come.

Acknowledgments

We thank two anonymous reviewers for their comments on the manuscript. Grounding line positions and ice velocities are available at the National Snow and Ice Data Center as part of the NASA MeASUREs project. Reconstruction of bed topography is available upon request from the authors until a finished, larger scale product is posted at NSIDC. This work was performed at the University of California Irvine and at the Jet Propulsion Laboratory, California Institute of Technology under a grant from the National Aeronautics and Space Administration's Cryospheric Science Program and Interdisciplinary Science Program.

The Editor thanks two anonymous reviewers for their assistance in evaluating this manuscript.

References

Favier, L., G. Durand, S. L. Cornford, G. H. Gudmundsson, O. Gagliardini, F. Gillet-Chaulet, T. Zwinger, A. J. Payne, and A. M. Le Brocq (2014), Retreat of Pine Island Glacier controlled by marine ice-sheet instability, *Nat. Clim. Change*, *4*, 117–121, doi:10.1038/nclimate2094.

Fretwell, P., et al. (2013), BEDMAP2: Improved ice bed, surface and thickness datasets for Antarctica, *The Cryosphere*, *7*, 375–393, doi:10.5194/tc-7-375-2013.

Gillet-Chaulet, F., and G. Durand (2010), Glaciology: Ice sheet advances in Antarctica, *Nature*, *467*, 794–795.

Gogineni, P. (2012), CReSIS RDS data, Digital Media, Lawrence, Kans. [Available at http://data.cresis.ku.edu/.]

Gudmundsson, G. H. (2013), Ice-shelf buttressing and the stability of marine ice sheets, *The Cryosphere*, *7*, 647–655, doi:10.5194/tc-7-647-2013.
Holt, J. W., D. D. Blankenship, D. L. Morse, D. A. Young, M. E. Peters, S. D. Kempf, T. G. Richter, D. G. Vaughan, and H. F. J. Corr (2006), New boundary conditions for the West Antarctic ice sheet: Subglacial topography of the Thwaites and Smith glacier catchments, *Geophys. Res. Lett.*, *33*, L09502, doi:10.1029/2005GL025561.
Jacobs, S. S., A. Jenkins, C. F. Giulivi, and P. Dutrieux (2011), Stronger ocean circulation and increased melting under Pine Island Glacier ice shelf, *Nat. Geosci.*, *4*, 519–523.
Jamieson, S. S. R., A. Vieli, S. J. Livingstone, C. Ó. Cofaigh, C. Stokes, C.-D. Hillenbrand, and J. A. Dowdeswell (2012), Ice-stream stability on a reverse bed slope, *Nature Geosci.*, *5*(11), 799–802.
Katz, R. F., and M. G. Worster (2010), Stability of ice-sheet grounding lines, *Proc. Roy. Soc. A*, *466*, 1597–1620.
Larour, E., H. Seroussi, M. Morlighem, and E. Rignot (2012), Continental scale, high order, high spatial resolution, ice sheet modeling using the Ice Sheet System Model (ISSM), *J. Geophys. Res.*, *117*, F01022, doi:10.1029/2011JF002140.
MacGrath, D., K. Steffen, H. Rajaram, T. Scambos, W. Abdalati, and E. Rignot (2012), Basal crevasses on the Larsen C Ice Shelf, Antarctica: Implications for meltwater ponding and hydrofracture, *Geophys. Res. Lett.*, *39*, L16504, doi:10.1029/2012GL052413.
Morlighem, M., E. Rignot, H. Seroussi, E. Larour, H. B. Dhia, and D. Aubry (2011), A mass conservation approach for mapping glacier ice thickness, *Geophys. Res. Lett.*, *38*, L19503, doi:10.1029/2011GL048659.
Morlighem, M., E. Rignot, J. Mouginot, X. Wu, H. Seroussi, E. Larour, and J. Paden (2013), High-resolution bed topography mapping of Russell Glacier, Greenland, inferred from Operation IceBridge data, *J. Glaciol.*, *59*, 1015–1023.
Mouginot, J., E. Rignot, and B. Scheuchl (2014), Sustained increase in ice discharge from the Amundsen Sea Embayment, West Antarctica, from 1973 to 2013, *Geophys. Res. Lett.*, *41*, 1576–1584, doi:10.1002/2013GL059069.
Park, J. W., N. Gourmelen, A. Shepherd, S. W. Kim, A. Vaughan, and D. G. Wingham (2013), Sustained retreat of the Pine Island Glacier, *Geophys. Res. Lett.*, *40*, 2137–2142, doi:10.1002/grl.50379.
Parizek, B. R., et al. (2013), Dynamic (in)stability of Thwaites Glacier, West Antarctica, *J. Geophys. Res. Earth Surf.*, *118*, 638–655, doi:10.1002/jgrf.20044.
Pritchard, H. D., R. J. Arthern, D. G. Vaughan, and L. A. Edwards (2009), Extensive dynamic thinning on the margins of the Greenland and Antarctic ice sheets, *Nature*, *461*, 971–975.
Rignot, E. (1998), Fast recession of a West Antarctic glacier, *Science*, *281*(5376), 549–551.
Rignot, E. (2001), Evidence for rapid retreat and mass loss of Thwaites Glacier, West Antarctica, *J. Glaciol.*, *47*(157), 213–222.
Rignot, E. (2008), Changes in West Antarctic ice stream dynamics observed with ALOS PALSAR data, *Geophys. Res. Lett.*, *35*, L12505, doi:10.1029/2008GL033365.
Rignot, E., J. L. Bamber, M. R. van den Broeke, C. Davis, Y. Li, W. J. van de Berg, and E. van Meijgaard (2008), Recent Antarctic ice mass loss from radar interferometry and regional climate modelling, *Nat. Geosci.*, *1*, 106–110.
Rignot, E., J. Mouginot, and B. Scheuchl (2011), Antarctic grounding line mapping from differential satellite radar interferometry, *Geophys. Res. Lett.*, *38*, L10504, doi:10.1029/2011GL047109.
Rignot, E., S. Jacobs, J. Mouginot, and B. Scheuchl (2013), Ice shelf melting around Antarctica, *Science*, *341*(6143), 266–270.
Schmeltz, M., E. Rignot, and D. McAyeal (2001), Ephemeral grounding as a signal of ice-shelf change, *J. Glaciol.*, *47*(156), 71–77.
Scott, J. B. T., G. H. Gudmundsson, A. M. Smith, R. G. Bingham, H. D. Pritchard, and D. G. Vaughan (2009), Increased rate of acceleration on Pine Island Glacier strongly coupled in gravitational driving stress, *The Cryosphere*, *3*, 125–131.
Thomas, R. H. (1973), The creep of ice shelves: Interpretation of observed behaviour, *J. Glaciol.*, *12*(64), 55–70.
Thomas, R. H., E. Rignot, P. Kanagaratnam, W. Krabill, and G. Casassa (2004a), Force-perturbation analysis of Pine Island Glacier suggests cause for recent acceleration, *Ann. Glaciol.*, *39*, 133–138.
Thomas, R. H., et al. (2004b), Accelerated sea-level rise from West Antarctica, *Science*, *306*, 255–258.
Vaughan, D. G., H. F. J. Corr, F. Ferraccioli, N. Frearson, A. O'Hare, D. Mach, J. W. Holt, D. D. Blankenship, D. L. Morse, and D. A. Young (2006), New boundary conditions for the West Antarctic ice sheet: Subglacial topography beneath Pine Island Glacier, *Geophys. Res. Lett.*, *33*, L09501, doi:10.1029/2005GL025588.
Velicogna, I., and J. Wahr (2006), Measurements of time-variable gravity shows a large mass loss in Antarctica, *Science*, *311*, 1754–1756.
Weertman, J. (1980), Bottom crevasses, *J. Glaciol.*, *25*(91), 185–188.
Wingham, D. G., D. W. Wallis, and A. Shepherd (2009), Spatial and temporal evolution of Pine Island Glacier thinning, 1995–2006, *Geophys. Res. Lett.*, *36*, L17501, doi:10.1029/2009GL039126.